



HAL
open science

Persistent random motion: uncovering cell migration dynamics

Daniel Campos, Vicenç Méndez, Isaac Llopis

► **To cite this version:**

Daniel Campos, Vicenç Méndez, Isaac Llopis. Persistent random motion: uncovering cell migration dynamics. *Journal of Theoretical Biology*, 2010, 267 (4), pp.526. 10.1016/j.jtbi.2010.09.022 . hal-00637813

HAL Id: hal-00637813

<https://hal.science/hal-00637813>

Submitted on 3 Nov 2011

HAL is a multi-disciplinary open access archive for the deposit and dissemination of scientific research documents, whether they are published or not. The documents may come from teaching and research institutions in France or abroad, or from public or private research centers.

L'archive ouverte pluridisciplinaire **HAL**, est destinée au dépôt et à la diffusion de documents scientifiques de niveau recherche, publiés ou non, émanant des établissements d'enseignement et de recherche français ou étrangers, des laboratoires publics ou privés.

Author's Accepted Manuscript

Persistent random motion: uncovering cell migration dynamics

Daniel Campos, Vicenç Méndez, Isaac Llopis

PII: S0022-5193(10)00496-0
DOI: doi:10.1016/j.jtbi.2010.09.022
Reference: YJTBI6162

To appear in: *Journal of Theoretical Biology*

Received date: 1 June 2010
Revised date: 14 September 2010
Accepted date: 15 September 2010

Cite this article as: Daniel Campos, Vicenç Méndez and Isaac Llopis, Persistent random motion: uncovering cell migration dynamics, *Journal of Theoretical Biology*, doi:[10.1016/j.jtbi.2010.09.022](https://doi.org/10.1016/j.jtbi.2010.09.022)

This is a PDF file of an unedited manuscript that has been accepted for publication. As a service to our customers we are providing this early version of the manuscript. The manuscript will undergo copyediting, typesetting, and review of the resulting galley proof before it is published in its final citable form. Please note that during the production process errors may be discovered which could affect the content, and all legal disclaimers that apply to the journal pertain.



www.elsevier.com/locate/jtbi

Persistent random motion: Uncovering cell migration dynamics

Daniel Campos*, Vicenç Méndez and Isaac Llopis

*Grup de Física Estadística. Departament de Física. Universitat Autònoma de
Barcelona, 08193 Bellaterra (Cerdanyola) Spain*

Abstract

In this paper we study analytically the stick-slip models recently introduced to explain the stochastic migration of free cells. We show that persistent motion of cells of many different types is compatible with stochastic reorientation models which admit an analytical mesoscopic treatment. This is proved by examining and discussing experimental data compiled from different sources in the literature, and by fitting some of these results too. We are able to explain many of the 'apparently complex' migration patterns obtained recently from cell tracking data, like power-law dependences in the mean square displacement or non-Gaussian behavior for the kurtosis and the velocity distributions, which depart from the predictions of the classical Ornstein-Uhlenbeck process.

* Corresponding author.

Email address: daniel.campos@uab.es (Daniel Campos).

1 Introduction

Studying the properties of cell movement is of fundamental interest to understand many physiological processes in living organisms (embryogenesis, wound healing, etc.) as well as their malfunctions (e.g. in tumors growth). Exhaustive research in this field is focused on the biophysical and biochemical intracellular processes driving cell signaling and motility. However, for many purposes like the analysis of tracking experiments or the implementation of migration algorithms into more general models, the use of phenomenological approaches as those based on stochastic processes is extremely helpful. Within this context, the Ornstein-Uhlenbeck (OU) process [1] has been considered for decades the archetypal model to describe persistent random motion of cells or other particles/organisms. This process is defined by the Langevin equation

$$\frac{d\mathbf{v}}{dt} = -\frac{1}{\tau}\mathbf{v} + \frac{\sqrt{2D}}{\tau}\boldsymbol{\xi}(t), \quad (1)$$

for the velocity vector \mathbf{v} , where $\boldsymbol{\xi}(t)$ represents a vector with white-noise components, D is the diffusion coefficient characteristic of Brownian motion, and the timescale τ is often called the persistence time. Fibroblasts locomotion [2], the motility of lung epithelial cells [3], microvessel endothelial cells [4] or self-motile colloids [5] are just some examples from the vast amount of systems which have been successfully interpreted in the light of this model. Even in recent studies where cells have been found experimentally to exhibit more complex migration patterns, the OU process is still the reference model to which more sophisticated approaches are compared [6–8].

The popularity of this approach is in part founded on the fact that the mean square displacement (MSD) and the velocity auto-correlation function (VACF)

of cells have been often experimentally observed to fit the behavior it predicts

$$\langle \mathbf{r}^2(t) \rangle = 2nD\tau \left(e^{-t/\tau} + t/\tau - 1 \right) \quad (2)$$

$$\langle \mathbf{v}(t)\mathbf{v}(0) \rangle = \frac{nD}{\tau} e^{-t/\tau} \quad (3)$$

where (2) is known as the Fürth formula [9] and n is the space dimension. Note that Eqs. (2-3) describe the behavior of averaged quantities, while much less efforts have been performed in order to verify directly Eq. (1) from experimental cell trajectories, since it requires much better resolution in data. Actually, the only systematic works conducted in that way we have found in the literature led to strong discrepancies between statistics from experimental trajectories and the OU process [8,10,11]. The results found in these References are that the acceleration perpendicular to the direction of motion exhibits zero-mean fluctuations, while the mean acceleration in the direction of motion decreases with the speed in a seemingly linear manner. The authors in [11] have already noted that the Fürth formula can also be derived from other models of persistent motion. So that, misinterpretations of cell migration dynamics can arise from assuming that there is an univocal equivalence between (2-3) and the OU process.

To illustrate these ideas let us consider a reorientation model which consists of a particle travelling with constant speed v_0 in a 2D space and whose orientation angle θ (which determines its direction of motion) exhibits white-noise fluctuations with a characteristic strength σ . For that situation, the microscopic equations of motion are

$$\frac{d\theta}{dt} = \sigma\xi(t) \quad \frac{d\mathbf{r}}{dt} = v_0\mathbf{u}_\theta \quad (4)$$

where $\mathbf{u}_\theta = (\cos \theta, \sin \theta)$ is a unit vector in the direction of motion and $\xi(t)$ is

white noise. One can now define the probability density $P(\mathbf{r}, \theta, t)$ of finding the particle at position \mathbf{r} with orientation θ at time t , given the initial conditions $\theta_0, \mathbf{r}_0 = (0, 0)$. Applying standard techniques from stochastic calculus [12], we can obtain the Fokker-Planck equation for the probability density P (see [13])

$$\frac{\partial P}{\partial t} = \frac{\sigma^2}{2} \frac{\partial^2 P}{\partial \theta^2} - v_0 \mathbf{u}_\theta \cdot \nabla P. \quad (5)$$

It is straightforward now to check from Eq. (5) that the MSD and the velocity auto-correlation of a particle governed by this model also satisfy Eqs. (2-3), with $\tau = 2/\sigma^2$, $D = 2v_0^2/\sigma^2$. So that it represents an alternative to the OU process for describing persistent motion (see [13,14] for some seminal papers on this field). The form of the first moments of P coincide for both models (1) and (4), but their microscopic differences become apparent for higher-order moments. For example, it is easy to check that the kurtosis $\langle \mathbf{r}^4(t) \rangle / \langle \mathbf{r}^2(t) \rangle^2$ is different in each model, though in both cases it tends to 3 for $t \rightarrow \infty$, as expected for a Gaussian variable.

Although it is not easy in general to elucidate the correct pattern of motion from experimental data, we think that the reorientation model has some advantages over the classical approach in Eq. (1). Firstly, it seems more natural to write the equations of motion in terms of the orientation coordinate θ (instead of using a fixed coordinate system), according to the results for the mean acceleration of cells reported in [8,11]. This will be specially appropriate for the case of nonisotropic particles (for example, rod-shaped), which move preferentially along one of their axis. Secondly, the simplicity of the reorientation model (4) makes generalizations of the model easier to implement, while generalizations of the OU process often involve memory kernels or other nontrivial effects. This has important implications on how experimental data

is interpreted, too. When the experimental results from cell trajectories are observed to depart from the predictions of the OU process, it is often interpreted as a trace of complexity at some level. Here, we explore simple and direct generalizations of the reorientation model which can explain many of these 'apparently complex' patterns of motion. Experimental data, obtained from different works previously published, will be used to support these ideas (Section 4).

2 Models overview

In this Section we summarize some of the different stochastic approaches that have been recently proposed to explain the dynamics of self-propelled particles (as is the case of cells in a diluted media). This will serve to put in context the stick-slip model that will be presented and developed in Section 3.

2.1 Model in which speed and direction fluctuate independently

The assumption made in Eq. (4) that the particles travel with constant speed can be relaxed by assuming instead that speed fluctuates around a mean value $\langle v \rangle$, giving rise to particles fluctuating both in their direction of motion and their absolute speed. This model has been proposed recently to explain the motion of propelled nanoparticles [15], but application to cell migration comes straightforward. Actually, the same idea had also been explored in the context of cell motion some years before [13], and similar models had already been used to explain migration of *Amoeba proteus* [16,17] (though the results in those works were mainly based in computer simulations).

Figure 1A describes schematically the microscopic behavior of a particle according to this model. The dotted lines represent the cell trajectory, in which changes of direction occur and the value of the speed changes at some instants (these instants are marked by crosses). As can be seen from the situation of the crosses, random changes in direction and speed are completely independent processes. As a consequence, one can study separately the fluctuations in speed and direction. If the cells are assumed to obey a certain velocity distribution $\rho(v)$ and the speed changes occur with a characteristic (constant) rate β then

$$\frac{\partial P(v, t)}{\partial t} = -\beta P(v, t) + \beta \rho(v) \quad (6)$$

gives us the evolution of $P(v, t)$, the probability density of particles traveling with speed v at time t .

Similarly, for the orientation angle θ (defined as in the Introduction Section), provided that orientation changes are smooth, one can use a diffusion approximation

$$\frac{\partial P(\theta, t)}{\partial t} = \kappa \frac{\partial^2 P(\theta, t)}{\partial \theta^2}. \quad (7)$$

where κ is the diffusion parameter for the fluctuations in the direction of motion.

The equations (6,7) can be exactly solved with the appropriate initial conditions. Since changes in speed and direction are independent, one has $P(v, \theta, t) = P(v, t) \cdot P(\theta, t)$. Then, from standard statistics in 2D one can compute, for instance, the mean distance travelled by the particle in this model $\langle |\mathbf{r}(\theta, t)| \rangle = \int_0^t dt' \int_0^\infty dv P(v, \theta, t') v$, or any moment $\langle r^n \rangle$, $\langle v^n \rangle$ of arbitrary order. So it is found that the MSD reads [15]

$$\begin{aligned} \langle \mathbf{r}^2(t) \rangle = & 2 \frac{\langle v^2 \rangle - \langle v \rangle^2}{(\kappa + \beta)^2} \left(e^{-(\kappa + \beta)t} + (\kappa + \beta)t - 1 \right) + \\ & + 2 \frac{\langle v \rangle^2}{\kappa^2} \left(e^{-\kappa t} + \kappa t - 1 \right). \end{aligned} \quad (8)$$

The first term in Eq. (8) represents Brownian motion arising from a particle with a fluctuating speed, while the second term accounts for rotational diffusion arising from the reorientation process.

For the VACF within this approach one obtains

$$\langle \mathbf{v}(t) \mathbf{v}(0) \rangle = \langle v \rangle^2 e^{-\kappa t} + \left(\langle v^2 \rangle - \langle v \rangle^2 \right) e^{-(\beta + \kappa)t} \quad (9)$$

which exhibits a double-exponential decay, compared to the single exponential one finds from the OU process.

2.2 Models with simultaneous fluctuations in speed and direction

In a recent work [18] two of the authors proposed a variation of the model in Section 2.1. According to it, the time instants at which the speed of the particle changes coincide with those where the direction changes (see Figure 1B). In the following, we will refer for simplicity to the models in Figures 1A and 1B as 'model A' and 'model B', respectively. So, model B corresponds to a motion pattern in which sojourns of constant speed are separated by (instantaneous) reorientation events. Though this is a relatively subtle modification of the previous model, the fact that now both types of fluctuations are not independent makes the present mathematical treatment quite different. In [18] we use the framework of Continuous-Time Random Walks (CTRW) to implement this idea (see [19] for a comprehensive review on such models). Within this framework one can derive an equation for the probability density $P(r, \theta, t)$. In

our specific case, this equation can only be explicitly written in the Fourier-Laplace space; so the transformation $P(r, \theta, t) \rightarrow P(q_x, q_y, \theta, s) \equiv \hat{P}$ is used, with q_x, q_y, s being the transform variables of x, y, t respectively. The evolution equation takes the form [18]

$$\frac{\sigma^2}{2} \frac{\partial^2 \hat{P}}{\partial \theta^2} = \left[s + iv (q_x \cos \theta + q_y \sin \theta) + \frac{v_D^2 (q_x \cos \theta + q_y \sin \theta)^2}{s + \beta + iv (q_x \cos \theta + q_y \sin \theta)} \right] \hat{P} - \frac{1}{2\pi} \quad (10)$$

where the parameter v_D measures the amplitude of the speed fluctuations. So, for $v_D = 0$ it is clear that (5) will be recovered after inverting by Fourier-Laplace.

From (10), the moments of $P(r, \theta, t)$ can also be found in a relatively easy way (see [18] or the Appendix for further details). The expressions for the MSD and the VACF one finds from (10) coincide with those from the model A (Eqs. (8) and (9)) after redefining the parameter κ as $\sigma^2 \beta$. As it happened with the two models discussed in the Introduction, these two approaches have the same first and second-order moments, but the microscopic differences between them (sketched in Figure 1) become evident for higher-order moments. The main advantage of this second approach based in the CTRW is that different extensions of the model can be implemented in a very natural way; this will be shown in Section 3.

2.3 Models with memory kernels

In comparison with the two previous approaches, where the microscopic details of the model (Figure 1) are absolutely clear, many other approaches used to fit experimental data on cell migration are based on the introduction of memory functions, or similar, into well established models, e.g. the OU process. One

example of this is the model presented in [10] and lately used in [8] to fit the spontaneous movements of *Dictyostelium* cells. This approach is based on the stochastic differential equations

$$\frac{d\mathbf{v}}{dt} = -\tau^{-1}(v(t))\mathbf{v} + \mu\mathbf{V}(t) + \sigma(v(t))\boldsymbol{\xi}(t) \quad (11)$$

$$\frac{d\mathbf{V}}{dt} = \mu\mathbf{v}(t) - \gamma\mathbf{V}(t) \quad (12)$$

where $\mathbf{V}(t)$ represents a memory function, whose time evolution is governed by (12), while μ and γ represent constant parameters. Note also that velocity-dependent friction (τ^{-1}) and noise memory functions (σ) have been introduced if compared with Eq. (1). All of these functions ($\mathbf{V}(t)$, $\sigma(v(t))$ and $\tau^{-1}(v(t))$) are to be adjusted from data fitting.

Though this kind of models provide excellent agreement to data, their drawback is that they require the help of mechanistic models or similar in order to justify the origin of such memory kernels so their hypothesis can be validated. The aim of our work, however, is not to criticize models based on kernels or memory effects, since the goodness of these models for fitting experimental data is clear. We just want to show that the experimental results can often be explained too by means of approaches like those in Sections 2.1 and 2.2, or direct generalizations of them. In those cases, memory effects are implicitly implemented through the time correlations introduced by the reorientation process. At this stage, we do not have any criteria to elucidate which of these approaches work better. We just think that reorientation models represent a simpler and intuitive alternative to models based on kernels. Besides, a complete analytical treatment is feasible for such models, which facilitates understanding.

3 Mesoscopic description for stick-slip models

The concept of stick-slip processes has been introduced recently in [11]. Actually, it corresponds to the "run and tumble" pattern long used to describe bacterial motion [20]. However, in order to stress the connection of our work with that in [11] we will rather use the term stick-slip.

In the original Reference [11], stick-slip processes have been introduced as a sort of numerical models (algorithms) able to implement realistically protrusion-retraction mechanisms responsible for cell migration. Here we will show that the CTRW formalism we used in [18] can be extended to implement these processes. By the analytical treatment of such models we expect to facilitate their understanding and check their validity for fitting cell data.

According to the discussion in the Section 2.2, we will consider a cell trajectory in 2D where the particle changes its direction of motion and absolute speed jointly at some time instants with a characteristic rate β , while σ is a measure of how much the orientation can change at each of these events. Now each reorientation event is assumed to last a finite random time, controlled by a constant characteristic rate β_2 . Regarding the distribution of speeds, we will consider here the simplest version of the model, in which the particle travels with constant speed v_0 during the motion periods. We think that the general model with an arbitrary distribution of velocities is also feasible analytically in the light of the velocity models proposed in [21]; that case, however, involves more complicated considerations, so we plan to deal with it in a separate forthcoming work.

Following the lines of CTRW models (see [18,19] and the references therein),

we define $P_i(\mathbf{r}, \theta, t)$ as the probability density for the particle to be located at position \mathbf{r} with orientation θ at time t . The label $i = 1$ stands for those particles waiting (while reorienting) at that position, while $i = 2$ denotes the particles in motion passing through that point. The total density of cells is then computed as $P = P_1 + P_2$. Also, we need to introduce $J_i(\mathbf{r}, \theta, t)$ as the probability density of particles with orientation θ that at time t stop moving at position \mathbf{r} ($i = 1$), and those which start moving at position \mathbf{r} after a waiting period ($i = 2$). The evolution of the model is then given by the system of mesoscopic equations

$$J_1(\mathbf{r}, \theta, t) = \int d\mathbf{r}' \int_0^{2\pi} d\theta' \int_0^t dt' J_2(\mathbf{r} - \mathbf{r}', \theta', t - t') T(\theta - \theta') \psi(\mathbf{r}', \theta', t') + \frac{\delta(\mathbf{r})\delta(t)}{2\pi} \quad (13)$$

$$J_2(\mathbf{r}, \theta, t) = \int_0^t dt' J_1(\mathbf{r}, \theta, t - t') \varphi(t') \quad (14)$$

$$P_1(\mathbf{r}, \theta, t) = \int d\mathbf{r}' \int_0^t dt' J_1(\mathbf{r}, \theta, t - t') \varphi^*(t') \quad (15)$$

$$P_2(\mathbf{r}, \theta, t) = \int d\mathbf{r}' \int_0^t dt' J_2(\mathbf{r} - \mathbf{r}', \theta, t - t') \psi^*(\mathbf{r}', \theta, t') \quad (16)$$

where we have assumed for simplicity that initially all the particles start waiting from position $\mathbf{r} = 0$ at $t = 0$ (see the last term in Eq. (13)). The first term on the right in (13) represents the contribution from those particles that started moving at time $t - t'$ with orientation θ' and then stop after covering a distance \mathbf{r}' in a travel time t' (according to the probability distribution $\psi(\mathbf{r}', \theta', t')$) and take a new orientation value θ according to the distribution $T(\theta - \theta')$. In Eq. (14) we apply the waiting times distribution $\varphi(t')$ for particles which stopped moving at time $t - t'$ and start moving again at time t . The distribution $\varphi^*(t')$ in (15) stands for the probability that the particle has not started moving yet after a waiting time t' . Finally, in (16) $\psi^*(\mathbf{r}', \theta, t')$ denotes the probability that a particle has not stopped after a time t' since it started moving, during which it has covered a distance \mathbf{r}' in the direction θ .

Since we have assumed in Section 3 that moving and waiting periods are governed by constant rates β and β_2 , respectively, we take the corresponding probability distribution functions to be exponential (that is, a Markov assumption). So that, for the constant speed case we have $\psi(\mathbf{r}, \theta, t) = \beta e^{-\beta t} \delta(\mathbf{r} - v_0 \mathbf{u}_\theta t)$ and $\varphi(t) = \beta_2 e^{-\beta_2 t}$, where \mathbf{u}_θ represents, as mentioned above, a unit vector in the direction of motion. Correspondingly, the other distributions will read $\psi^*(\mathbf{r}, \theta, t) = e^{-\beta t} \delta(\mathbf{r} - v_0 \mathbf{u}_\theta t)$ and $\varphi^*(t) = e^{-\beta_2 t}$. For further details on this kind of models, the reader is addressed to the References [18,22,23].

For the case of a smooth reorientation process (smooth changes in θ), the closed equations for P_1 and P_2 can be easily found and solved in the Fourier-Laplace space (all the details are given in the Appendix). The moments of these distributions can thus be found easily; for instance, we obtain for the ensemble-averaged MSD

$$\langle \mathbf{r}^2(t) \rangle = \int_0^{2\pi} d\theta \int \mathbf{r}^2 P(\mathbf{r}, \theta, t) d\mathbf{r} = 2v_0^2 \left(p_0(t) + p_1(t)e^{-\lambda_1 t} + \sum_{k=2}^5 p_k e^{-\lambda_k t} \right) \quad (17)$$

where the functions $p_0(t)$, $p_1(t)$ are first-order polynomials in t and the p_k 's (for $k = 2 \dots 5$) are independent of t (the exact expressions for all of them are provided in the Appendix). Likewise, the characteristic exponents λ_k read

$$\begin{aligned} \lambda_1 &= \beta + \beta_2 \\ \lambda_2 &= \frac{1}{2} \left(\beta + \beta_2 + \sqrt{(\beta + \beta_2)^2 - 4\beta\beta_2\sigma^2} \right) \\ \lambda_3 &= \frac{1}{2} \left(\beta + \beta_2 - \sqrt{(\beta + \beta_2)^2 - 4\beta\beta_2\sigma^2} \right) \\ \lambda_4 &= \frac{1}{2} \left(\beta + \beta_2 + \sqrt{(\beta + \beta_2)^2 - 4\beta^2\sigma^2} \right) \\ \lambda_5 &= \frac{1}{2} \left(\beta + \beta_2 - \sqrt{(\beta + \beta_2)^2 - 4\beta^2\sigma^2} \right). \end{aligned} \quad (18)$$

From Eq. (17) and the explicit expression for $p_0(t)$ (see (32)) one finds out

how the asymptotic diffusion coefficient depends on the characteristics rates in the model

$$D \equiv \lim_{t \rightarrow \infty} \frac{\langle \mathbf{r}^2(t) \rangle}{4t} = \frac{v_0^2}{\beta \sigma^2} \left(\frac{\beta_2}{\beta + \beta_2} \right)^2. \quad (19)$$

On the other side, the VACF can be evaluated from (17) (since the motion process is isotropic) by applying the Green-Kubo relation [24]

$$\frac{d \langle (x(t) - x(t_0))^2 \rangle}{dt_0} = 2 \int_{t_0}^t \langle v_x(t') v_x(t_0) \rangle dt' \quad (20)$$

to each Cartesian coordinate, and evaluating this at $t_0 = 0$, $\mathbf{r}(t_0) = 0$. That calculation must be carried out only for the particles in state 2 (that is, for $P_2(\mathbf{r}, \theta, t)$), since particles in the state 1 have zero speed. The corresponding result has the general form

$$\langle \mathbf{v}(t) \mathbf{v}(0) \rangle = v_0^2 \left(m_1(t) e^{-\lambda_1 t} + \sum_{k=2}^3 m_k e^{-\lambda_k t} \right), \quad (21)$$

where again $m_1(t)$ is a first-order polynomial, and m_2, m_3 are constant parameters (combination of the p_k 's). Although these are quite lengthy expressions, the interesting feature from the results (17,21) is that they tell us that the global dynamics of this stick-slip process is basically governed by up to 5 different timescales λ_k^{-1} (with $k = 1 \dots 5$) in the case of the MSD, or just 3 for the case of the VACF. From that point of view, the stick-slip model considered here involves an increasing level of complexity compared to the models A and B, albeit the number of parameters in the model is the same (four) in both cases (namely $v_0, \beta, \beta_2, \sigma^2$). Obviously, introducing here an arbitrary distribution of speeds would increase this complexity even more. Note, however, that Monte Carlo simulations of this process were conducted in [11] and the VACF was fitted there just to a double-exponential (see Figure 5 in that Reference). This is because for many choices of the parameters, two (or even the three) of

the timescales in (21) could take similar values and so in general they cannot be distinguished graphically.

4 Experimental data for cell migration

In this Section we will try to show how reorientation models, as the stick-slip case introduced in the previous Section, can explain many of the departures from the OU process that have been found recently in different cell migration experiments. To complete our discussion we will also compare with the results obtained from the models A and B. We will discuss different parameters reported in experimental works and will try to fit the experimental data to the stick-slip process presented here. For such fitting procedure we will mainly use the data collected in [8] for vegetative and starved (after 5.5 hours) *Dicystelium discoideum* cells (since this is one of the most exhaustive works we have found in the literature), plus some data from References [6] and [11].

a) Mean-square displacement. This is probably the most recurrent parameter in studies on cell migration. The OU process predicts, according to (2), a transition from ballistic to diffusive behavior which occurs at timescale τ . However, departures from that formula have increasingly appeared during the last years. Most of these departures consist of a power-law scaling of the type $\langle \mathbf{r}^2(t) \rangle \sim t^\alpha$ [6,8,25–27]. This easily connects with the theory of anomalous diffusion, which is very popular among theoreticians at present [19], so concepts like 'Levy flight' or 'long-range memory' are now relatively common within this field. According to theoretical works, anomalous diffusion has different origins: i) long-range time correlations exist in the particles dynamics, which can be a consequence of different internal or external mechanisms, or ii)

movement constraints are imposed by heterogeneous (fractal-like) media [28] or by crowding effects [29]. In most works where power-law dependences of the MSD have been found, the influence of external mechanisms or constraints has been minimized. Thus, the only explanation seems to be that internal mechanisms in the cell should be responsible for the emergence of memory effects; this has been the interpretation suggested by most of the authors. However, this idea is quite speculative, since experimental evidence for these long-range memory mechanisms is scarce, in the best case. According to that, we can ask: 'Is there an alternative to explain why these power-law dependences are observed so often without invoking such concepts from anomalous diffusion?'. In our opinion a positive answer can be provided by the reorientation models studied here (alternative answers have also been explored in the literature: for example, it has been recently shown [30] that heterogeneous diffusivities in a set of individual particles can lead statistically to the emergence of anomalous diffusion at the ensemble level).

For the models depicted in Figure 1 the form of the MSD is given by (8). According to that, the MSD will be mainly determined by the relative values of the characteristic rates β and κ . For $\beta \ll \kappa$, the formula is completely governed by κ and so a single *ballistic-to-diffusive* transition will be found, as in the OU process. For $\beta \gg \kappa$ two transitions at very different timescales (one for each term in (8)) occur, so we observe a sequence *ballistic-diffusive-ballistic-diffusive* [15]. Interestingly, for intermediate values of β the MSD often fits quite well a power-law dependence $\langle \mathbf{r}^2(t) \rangle \sim t^\alpha$ with an exponent α which lies between 1 and 2. Exactly the same behavior holds for the expression (17) we have derived for the stick-slip model.

These results for the MSD have been discussed in detail in [18], where they

have been used to interpret data from experiments with nanoparticles. Our hypothesis is that the same could apply to cell migration data, so some of the experimental works where anomalous diffusion has been reported could actually correspond to a behavior like that in (8). There are some facts that seem to support this idea:

- i) The values of the anomalous exponents α found experimentally (in the absence of crowding or geometrical constraints) are always between 1 and 2.
- ii) The power-law tails in the MSD often extend over just one or two decades of time values (in the best case) due to experimental limitations. So, it is not clear that the asymptotic regime has been reached yet.

By 'asymptotic regime' we mean here that the observational times have reached the condition $t \gg \kappa^{-1}$, where diffusive behavior should be recovered. This condition is equivalent to the '*criterion for distinguishing true superdiffusion from correlated random-walks*' given in [31]. The authors in that Reference already detected the formal problem reported here and discuss its implications on the analysis of cell motility data as well as for foraging in animals. So, this controversy between anomalous or 'similar to anomalous' is not a new problem.

Our hypothesis is tested by fitting the experimental data from [8] to the result (17) and to the models A and B (Eq. (8)). Figure 2 (left) shows that both models (solid and dotted lines, respectively) can fit reasonably well the experimental results, though apparently the data seems to exhibit a power-law dependence (as claimed originally by the authors in [8]). For the sake of completeness, we also show the data fitting corresponding to the MSD results in [6]. We stress, however, that from this fitting procedure it is very difficult to determine which models fits the data best; anyway, this is not the aim of our

paper. To perform such a detailed study it would be necessary to have access to the original raw data, and even in that case it is unlikely that concluding results could be found.

b) Velocity autocorrelation function. We have already shown the results for the VACF one obtains in the stick-slip model (Eq. (21)) and for reorientation models A and B (Eq. (9)). Such multi-exponential functions are able to explain all the results of cell migration in 2D we have found in the literature. For example, this double-exponential behavior has been explicitly observed in experiments for HaCaT cells, dermal keratinocytes or different developmental stages of *Dictyostelium discoideum* [8,10,11,32]. The single exponential decay found in other works will be recovered when fluctuations in the speed are much larger than fluctuations in the direction ($\beta \ll \kappa$). Also, in those cases when the time resolution of observations is not good enough to reproduce accurately the region $t \ll (\beta + \kappa)^{-1}$, it will be impossible to observe experimentally the second exponential term and a single exponential will be found. The only exception is the case reported in [6], where the migration of epithelial Madin-Carby canine kidney cells has been investigated. There, a power-law scaling for the VACF has been observed. However, this behavior is found barely over one decade of time values (see Figure 3 in [6]), so it is plausible that other curves could be able to fit well the data, too.

The comparison between Eq. (21) (stick-slip model), Eq. (9) (obtained from models A or B) and the data for *Dictyostelium* cells obtained from the experimental setting in References [8] and [11] shows an excellent agreement too (Figure 2, right and Figure 4, respectively). This reinforces the main idea of the present paper, which is to show that stochastic reorientation models provide an alternative description to cell migration patterns. Note that in Figure 2 we

have fitted simultaneously the MSD and the VACF just with the 4 parameters of our model (see Figure Caption); the agreement found can be interpreted as a verification of the Green-Kubo formula (20). More free parameters were used in the original Reference [8] for the same fitting, though it must be noted that the authors there also fitted the behavior of the cell acceleration as a function of the velocity (this cannot be done in our case since we are not using a Langevin description).

c) Kurtosis. Another parameter of special interest is the kurtosis $\langle \mathbf{r}^4(t) \rangle / \langle \mathbf{r}^2(t) \rangle^2$.

It is known that this parameter must tend to 3 for a diffusive regime characterized by a Gaussian distribution. This is not true, however, for anomalous diffusion, since in that case the classical central limit theorem no longer applies. Unfortunately, the values of the kurtosis as a function of time are only available for two of the references discussed throughout this paper [6,8]. In the former [6] the asymptotic behavior of the kurtosis was found to tend asymptotically to the value 2.3. This has been interpreted as a departure from Brownian models, and so by the existence of a long-range memory effect. In the latter [8], the tendency of the kurtosis towards 3 as $t \rightarrow \infty$ is found (note that in [8] the kurtosis is defined as $\langle \mathbf{r}^4(t) \rangle / \langle \mathbf{r}^2(t) \rangle^2 - 3$ so there is a shift in the results there). However, this asymptotic value is reached from above which is a departure from the OU process, where the kurtosis is a monotonically increasing function [1].

In fact, we show now that both results can be explained (qualitatively, at least) from our reorientation models. Using the same calculation methods as reported in [18] and [15], the fourth moment $\langle \mathbf{r}^4(t) \rangle$ can be calculated for the stick-slip model and the two other models considered here. However, the corresponding expressions one obtains are huge so we cannot reproduce them here; we just

show the corresponding plots for some arbitrary parameters (Figure 5). Note that the two models in Figure 1 yield now different results, since (as stated above) the microscopic differences between them become apparent for higher-order moments.

Figure 5 confirms that the kurtosis exhibits a non-monotonic behavior which is in a qualitative agreement with the results in [6,8]. Also, the stick-slip model presented here is able to explain asymptotic deviations from the value 3 expected for Gaussian variables (Figure 5, right). In summary, this shows that there is no need to account for memory effects or long tailed distributions to explain such results. We must admit that a quantitative agreement with experimental data, using the parameter values obtained from the fitting in Figure 2, has been tried and the results are quite poor, specially for short times (Figure 6). Note, however, that the models proposed in the References [6,8] were not able to fit the short and intermediate-time regime for the kurtosis, neither. This is in fact a usual problem, which may be due to the fact that discretization in data acquisition (both in time and space) strongly affect the kurtosis values, specially for small times. This is another aspect of extreme importance which requires further investigation [27].

d) Speed and velocity distributions. In the reorientation models considered here the speed probability distribution is a model input, so it cannot be used to fit the experimental data; however, it is convenient to include some comments about it. Usually, a standard assumption is to consider a Gaussian distribution for v . However, several works have reported experimental evidence of non-Gaussian (exponential or power-law-like) tails for these distributions. To be more specific, one of the components of the velocity (for example, v_x) is observed to exhibit this unexpected behavior [8,10,25,26,33]. This is clearly a

departure from the OU process, where all the components of the velocity are Gaussian variables. Instead, note this does not happen for the reorientation models explored here. If one wants to find for the reorientation model the probability distribution $Q(v_x)$ of the velocity component $v_x = v \cos \theta$, this can be done easily from probability theory. The formula [34]

$$Q(z) = \int_{-\infty}^{\infty} f\left(x, \frac{z}{x}\right) \frac{1}{|x|} dx \quad (22)$$

allows one to find the probability distribution of the product $Z = XY$ of two random variables X, Y , with $f(x, y)$ being the joint distribution of these two variables. For any reorientation model without a preferential direction of motion, it can be assumed that the distribution of the θ values is uniform, which leads to a probability distribution $\sim (1 - \cos^2 \theta)^{-1/2}$ for the variable $\cos \theta$. Using this result and assuming a Gaussian distribution $\sim e^{-\gamma v^2}$ for the speed, with a characteristic exponent γ , the Equation 22 can be applied. It leads to the analytical solution

$$Q(v_x) \sim e^{-\frac{\gamma v_x^2}{2\pi}} K_0\left(\frac{\gamma v_x^2}{2\pi}\right) \quad (23)$$

where $K_0()$ denotes the modified Bessel function of zeroth order. Clearly, the expression (23) exhibits a non-Gaussian behavior for small and intermediate times (in general it resembles very much an exponential decay). At long times, however, it will tend to a Gaussian distribution, as the central limit theorem requires. So, we see that, provided our window of experimental times cannot reach the asymptotic regime $t \gg \kappa^{-1}$ an exponential decay of the velocities will be found, as observed in [10,33]. This cannot explain, however, why power-law tails have been observed in other experimental works. In those works, it seems that cell interactions were important (this happens for example in the case of Hydra cells studied in [25]), while our approach here is restricted to free cells.

In other cases, velocities are computed from measuring the cell displacements at scales smaller than the cell size [8]. For those observations cell deformation is expected to play a major role in the short-time dynamics, so biomechanical or mixed approaches [35] may be then more appropriate.

5 Conclusions

A reorientation model, equivalent to the stick-slip process introduced recently in [11] has been presented and analytically explored from a mesoscopic CTRW formalism in order to show its interest for cell migration. In addition, we have provided an extensive review of those experimental works on cell migration where departures from the OU process have been detected. By analyzing one by one the main statistical parameters measured in those works we have been able to show that our stochastic reorientation models are compatible with most of the results observed. Again, we do not mean that motion of cells must correspond necessarily to such microscopic patterns. Basically the contribution of our work lies in showing that many departures from the OU process, which had been previously attributed to memory kernels or other complex effects, also admit a simpler interpretation. Since biological systems have multiple and complex internal states, we think there is a great value in identifying non-uniqueness in models that can describe experimental data. Models based on memory kernels, as discussed in Section 2, rely on the hypothesis that the interactions between the cells and the surrounding media leads to the appearance of some specific memory effects, which requires justification from biophysical (mechanistic) models. The approach presented here avoids that drawback. Besides, the results obtained in [11,8], where the Langevin Equation

(1) has been tested directly, seem to support our general idea that reorientation models represent a more appropriate way to describe cell motion.

While our approach can provide a quite general framework for the persistent motion of free cells at low densities, it is clear that more complex situations involving cell interactions or external stimuli are out of the scope of the present work. More sophisticated approaches will be required for those situations, and it is not clear yet if the CTRW formalism used here will be useful still in that case. Note, for example, that even extremely simple interactions between particles can lead to quite complicated collective and cooperative phenomena, a topic which is at present under investigation (see [36] and the references therein).

Anyway, even for the noninteracting particles considered here many questions remain open. For example: if stochastic reorientation can really explain most of cell migration patterns, do then these patterns correspond to any functional advantage as an optimal search strategy (in the line of the results reported in [37])? Is it really possible to describe the short-time dynamics of cell migration (which is rather dominated by cell deformations) just by stochastic approaches based in point particles? How does the time-discretization introduced in data acquisition affect all these results? These questions are just to illustrate that understanding cell migration patterns still represents a really challenging task.

6 Appendix

The system of Eqs. (13-16) can be explicitly solved for some particular cases in order to reach an expression for the MSD. Introducing all the probability

distribution functions given in the text into (13-16), and transforming from the real coordinates (\mathbf{r}, t) to Fourier-Laplace coordinates $(q_x, q_y, s) = (\mathbf{q}, s)$, this system of equations takes the much more manageable form

$$\widehat{J}_1(\mathbf{q}, \theta, s) = \int_0^{2\pi} d\theta' \frac{\beta T(\theta - \theta')}{s + \beta + iv_0 [q_x \cos(\theta') + q_y \sin(\theta')]} \widehat{J}_2(\mathbf{q}, \theta', s) + \frac{1}{2\pi} \quad (24)$$

$$\widehat{J}_2(\mathbf{q}, \theta, s) = \frac{\beta_2}{s + \beta_2} \widehat{J}_1(\mathbf{q}, \theta, s) \quad (25)$$

$$\widehat{P}_1(\mathbf{q}, \theta, s) = \frac{1}{s + \beta_2} \widehat{J}_1(\mathbf{q}, \theta, s) \quad (26)$$

$$\widehat{P}_2(\mathbf{q}, \theta, s) = \frac{1}{s + \beta + iv_0(q_x \cos \theta + q_y \sin \theta)} \widehat{J}_2(\mathbf{q}, \theta, s) \quad (27)$$

where we use the hat $(\widehat{\cdot})$ to denote the Fourier-Laplace transform. In the following, we will obviate for simplicity the explicit dependence of \widehat{J} and \widehat{P} in their variables. Now, if we assume that orientation changes are smooth we can expand (24) for $\theta \rightarrow \theta'$, which yields up to second order

$$\widehat{J}_1 = \left(1 + \sigma^2 \frac{\partial^2}{\partial \theta^2}\right) \frac{\beta}{s + \beta + iv_0(q_x \cos \theta + q_y \sin \theta)} \widehat{J}_2 + \frac{1}{2\pi} \quad (28)$$

where $\sigma^2 \equiv \frac{1}{2} \int_0^{2\pi} \theta^2 T(\theta)$ is the variance of the distribution $T(\theta)$, a measure of how much the orientation θ can be changed. Note also that we have assumed in Eq. (28) the orientation process to be isotropic, so $\int_0^{2\pi} \theta T(\theta) = 0$. Now, we can obtain from the system of Eqs. (25-28) the closed expressions for the density distributions \widehat{P}_1 and \widehat{P}_2 :

$$0 = \beta \sigma^2 \frac{\partial^2 \widehat{P}_2}{\partial \theta^2} + \left(\beta - \frac{s + \beta_2}{\beta_2} [s + \beta + iv_0(q_x \cos \theta + q_y \sin \theta)] \right) \widehat{P}_2 + \frac{1}{2\pi} \quad (29)$$

$$\widehat{P}_1 = \frac{s + \beta + iv_0(q_x \cos \theta + q_y \sin \theta)}{\beta_2} \widehat{P}_2 \quad (30)$$

These equations can be formally inverted to the real coordinates (\mathbf{r}, t) but a solution for $P_1(\mathbf{r}, \theta, t)$, $P_2(\mathbf{r}, \theta, t)$ cannot be explicitly found. However, the MSD is easier to compute in the Fourier-Laplace coordinates from $\langle \mathbf{r}^2(s) \rangle =$

$-\left[\frac{\partial^2 \widehat{P}}{\partial q_x^2} + \frac{\partial^2 \widehat{P}}{\partial q_y^2}\right]_0$, where $\widehat{P} = \widehat{P}_1 + \widehat{P}_2$ and the subindex $_0$ denotes that the function is being evaluated at $q_x = 0, q_y = 0$. In [18] we have provided an easy method for doing this. First we find $[\widehat{P}_1]_0$ and $[\widehat{P}_2]_0$ by solving (29-30), integrating then over θ and imposing the particle conservation condition $[P_1 + P_2]_0 = \frac{1}{2\pi s}$. Next, we differentiate (29-30) with respect to q_x and use the previous result to find $\left[\frac{\partial \widehat{P}_1}{\partial q_x}\right]_0$ and $\left[\frac{\partial \widehat{P}_2}{\partial q_x}\right]_0$, and we do the same for q_y . By repeating this procedure again, we finally find

$$\langle \mathbf{r}^2(s) \rangle = \frac{2v_0^2(s + \beta_2)^2}{s^2(s + \beta + \beta_2)^2} \left(\frac{\beta_2}{s^2 + (\beta + \beta_2)s + \beta\beta_2\sigma^2} + \frac{s + \beta}{s^2 + (\beta + \beta_2)s + \beta^2\sigma^2} \right). \quad (31)$$

This expression, inverted from the Laplace coordinate s back to t , takes finally the form given in Eq. (17). For the sake of completeness, we provide the exact expressions of the p_k 's one obtains so:

$$\begin{aligned}
 p_0(t) &= \frac{2\beta_2 \left[(\beta + \beta_2)^3 + \sigma^2\beta(2\beta^2 + \beta_2^2 + 3\beta\beta_2) + 2\beta_2\beta^2\sigma^2(\beta + \beta_2)t \right]}{\beta^3\sigma^4(\beta + \beta_2)^3} \\
 p_1(t) &= \frac{-2 \left[\beta(2\beta_2^3 - \beta^3) + \beta_2(\beta_2^3 - 2\beta^3) - \beta\beta_2\sigma^2(\beta^2 + 1\beta_2^2 + 3\beta\beta_2) + \beta^2\beta_2\sigma^2(\beta^2 - \beta_2^2)t \right]}{\beta^2\beta_2\sigma^4(\beta + \beta_2)^3} \\
 p_2 &= \frac{2\beta\beta_2(1 + \sigma^2) - 2\lambda_3(\beta - \beta_2)}{\beta^2\beta_2\sigma^4(2\lambda_3 - \beta - \beta_2)} \\
 p_3 &= \frac{2\beta\beta_2(1 + \sigma^2) - 2\lambda_2(\beta - \beta_2)}{\beta^2\beta_2\sigma^4(2\lambda_2 - \beta - \beta_2)} \\
 p_4 &= \frac{2\lambda_4(\beta_2 - \beta\sigma^2)}{\beta^3\sigma^4(2\lambda_4 - \beta - \beta_2)} \\
 p_5 &= \frac{2\lambda_5(\beta_2 - \beta\sigma^2)}{\beta^3\sigma^4(2\lambda_5 - \beta - \beta_2)} \quad (32)
 \end{aligned}$$

Acknowledgements

This research has been partially supported by Grants Nos. CGL 2007-60797 (DC), FIS 2009-13370-C02-01 (VM) and SGR 2009-00164 .

References

- [1] Uhlenbeck, G.E. and L.S. Ornstein. 1931 On the Theory of Brownian Motion. *Phys. Rev.* 36:823-841.
- [2] Gail, M.H. and C.W. Boone. 1970 The Locomotion of Mouse Fibroblasts in Tissue Culture. *Biophys. J.* 10:980-993.
- [3] Wright, A., Y.-H. Li and C. Zhu. 2008 The Differential Effect of Endothelial Cell Factors on in vitro Motility of Malignant and non-malignant Cells. *Ann. Biomed. Eng.* 36:958-969.
- [4] Stokes, C.L., D.A. Lauffenburger and S.K. Williams. Migration of individual microvessel endothelial cells: stochastic model and parameter measurement. *J. Cell Sci.* 99:419-430 (1991).
- [5] Howse, J.R., R.A.L. Jones, A.J. Ryan, T. Gough, R. Vafabakhsh and R. Golestanian. 2007 Self-Motile Colloidal Particles: From Directed Propulsion to Random Walk. *Phys. Rev. Lett.* 99: 048102.
- [6] Dieterich, P., R. Klages, R. Preuss and A. Schwab. 2008 Anomalous dynamics of cell migration. *Proc. Natl. Acad. Sci. USA* 105:459-463.
- [7] Li, L., S.F. Norrelykke and E.C. Cox. 2008 Persistent Cell Motion in the Absence of External Signals: A Search Strategy for Eukaryotic Cells. *PLoS One* 3:e2093.
- [8] Takagi, H., M.J. Sato, T. Yanagida and M. Ueda. 2008 Functional Analysis of Spontaneous Cell Movement under Different Physiological Conditions. *PLoS One* 3:e2648.
- [9] Fürth, R. 1920 *Zeits f. Physik* 2:244.
- [10] Selmeczi, D., S. Mosler, P.H. Hagedorn, N.B. Larsen and H. Flyvbjerg. 2005 Cell Motility as Persistent Random Motion: Theories from Experiments. *Biophys. J.* 89:912-931.

- [11] Selmeczi, D., L. Li, L.I.I. Pedersen, S.F. Nrrclykke, P.H. Hagedorn, S. Mosler, N.B. Larsen, E.C. Cox and H. Flyvbjerg. 2008 Cell motility as random motion: A review. *Eur. Phys. J. Special Topics* 157:1-15.
- [12] Gardiner, C.W. 2004 *Handbook of Stochastic Methods for Physics, Chemistry and the Natural Sciences*, 3rd Ed. Berlin: Springer.
- [13] Schienbein, M. and H. Gruler. 1993. Langevin Equation, Fokker-Planck Equation and Cell Migration. *Bull. Math. Biol.* 55:585-608.
- [14] Othmer, H.G., S.R. Dunbar and W. Alt. 1988. Models of dispersal in biological systems. *J. Math. Biol.* 26:263-298.
- [15] Peruani, F. and L.G. Morelli. 2007 Self-Propelled Particles with Fluctuating Speed and Direction of Motion in Two Dimensions. *Phys. Rev. Lett.* 99:010602.
- [16] Miyoshi, H., N. Masaki and Y. Tsuchiya. 2003 Characteristics of trajectory in the migration of *Amoeba proteus*. *Protoplasma* 222:175-181.
- [17] Masaki, N., H. Miyoshi and Y. Tsuchiya. 2007 Characteristics of motive force derived from trajectory analysis of *Amoeba proteus*. *Protoplasma* 230:69-74.
- [18] Campos, D. and V. Méndez. 2009 Superdiffusive-like motion of colloidal nanorods. *J. Chem. Phys.* 130:134711.
- [19] Metzler, R. and J. Klafter. 2000 The Random Walk's Guide to Anomalous Diffusion: a Fractional Dynamics Approach. *Phys. Rep.* 339:1-77.
- [20] Berg, H.C. 2004 *E. Coli in Motion*. New York: Springer.
- [21] Zaburdaev, V., M. Schmiedeberg and H. Stark. 2008 Random walks with random velocities. *Phys. Rev. E* 78:011119.
- [22] Zumofen, G. and J. Klafter. 1993 Scale-invariant motion in intermittent chaotic systems. *Phys. Rev. E* 47:851-863.

- [23] Méndez, V., D. Campos and S. Fedotov. 2004 Front propagation in reaction-dispersal models with finite jump speed. *Phys. Rev. E* 70:036121.
- [24] Kubo, R., M. Toda and N. Hashitsume. 1991 *Statistical physics II, Nonequilibrium statistical mechanics*, 2nd Ed. Berlin: Springer.
- [25] Upadhyaya, A., J.-P. Rieu, J.A. Glazier and Y. Sawada. 2001 Anomalous diffusion and non-Gaussian velocity distribution of *Hydra* cells in cellular aggregates. *Physica A* 293:549-558.
- [26] Thurner, S., N. Wick, R. Hanel, R. Sedivy and L. Huber. 2003 Anomalous diffusion on dynamical networks: a model for interacting epithelial cell migration. *Physica A* 320:475-484.
- [27] Potdar, A.A., J. Lu, J. Jeon, A.M. Weaver and P.T. Cummings. 2009. Bimodal Analysis of Mammary Epithelial Cell Migration in Two Dimensions. *Ann. Biomed. Eng.* 37:230-245.
- [28] Ben-Avraham, D. and S. Havlin. *Diffusion and reactions in fractals and disordered systems*. Cambridge Univ. Press (Cambridge, 2005).
- [29] Banks, D.S. and C. Fradin. 2005 Anomalous Diffusion of Proteins Due to Molecular Crowding. *Biophys. J.* 89:2960-2971.
- [30] S. Hapca, J.W. Crawford and I. M. Young. 2009 Anomalous diffusion of heterogeneous populations characterized by normal diffusion at the individual level. *J. R. Soc. Interface* 6:111-122.
- [31] Viswanathan, G.M., E.P. Raposo, F. Bartomeus, J. Catalan and M.G.E. da Luz. 2005 Necessary criterion for distinguishing true superdiffusion from correlated random walk processes. *Phys. Rev. E* 72:011111.
- [32] Maeda, Y.T., J. Inose, M.Y. Matsuo, S. Iwaya and M. Sano. 2008 Ordered Patterns of Cell Shape and Orientational Correlation during Spontaneous Cell Migration. *PLoS One* 3:e3734.

- [33] Czirák, A., K. Schlett, E. Madarász and T. Vicsek. 1998 Exponential Distribution of Locomotion Activity in Cell Cultures. *Phys. Rev. Lett.* 81:3038-3041.
- [34] Rohatgi, V.K. 1976 *An Introduction to Probability Theory and Mathematical Statistics*. New York: Wiley.
- [35] Ohta, T. and T. Ohkuma. 2009 Deformable Self-Propelled Particles. *Phys. Rev. Lett.* 102:154101.
- [36] F. Ginelli, F. Peruani, M. Bar and H. Chaté. 2010 Large-Scale Collective Properties of Self-Propelled Rods. *Phys. Rev. Lett.* 104:184502.
- [37] Friedrich, B.M. 2008 Search along persistent random walks. *Phys. Biol.* 5:026007.

Figure captions

Figure 1.

Random-walk representation of the model in [15] (Model A) and in [18] (Model B). The dotted lines represent the trajectory of a particle, and the crosses are the random instants at which it changes the value of speed.

Figure 2.

Comparison between the results from the stick-slip model presented here (solid lines), the models A and B (dotted lines) and the experimental data extracted from [8] for vegetative and starved *Dictyostelium* cells (symbols, see Legends). A simultaneous fitting for the MSD and the VACF data has been performed. The fitted parameters are, for the stick-slip model, $\beta = 2.56 \text{ s}^{-1}$, $\beta_2 = 3.64 \text{ s}^{-1}$,

$\sigma = 0.62$, $v_0 = 6.80 \mu\text{m/s}$ (vegetative cells) and $\beta = 2.11 \text{ s}^{-1}$, $\beta_2 = 3.91 \text{ s}^{-1}$, $\sigma = 0.48$, $v_0 = 16.5 \mu\text{m/s}$ (starved cells). For the other case we obtain $\beta = 4.87 \text{ s}^{-1}$, $\kappa = 0.64 \text{ s}^{-1}$, $\langle v \rangle = 2.52 \mu\text{m/s}$, $\langle v^2 \rangle = 20.6 \mu\text{m}^2/\text{s}^2$ (vegetative cells) and $\beta = 12.31 \text{ s}^{-1}$, $\kappa = 0.30 \text{ s}^{-1}$, $\langle v \rangle = 9.79 \mu\text{m/s}$, $\langle v^2 \rangle = 376.7 \mu\text{m}^2/\text{s}^2$ (starved cells).

Figure 3.

MSD comparison between the results from the stick-slip model presented here (solid lines), the models A and B (dotted lines) and the experimental data extracted from [6] for Madin-Darby canine kidney cell strains of the wild type and NHE-deficient (symbols, see Legend). The fitted parameters are, for the stick-slip model, $\beta = 1.08 \text{ s}^{-1}$, $\beta_2 = 0.19 \text{ s}^{-1}$, $\sigma = 0.36$, $v_0 = 1.19 \mu\text{m/s}$ (wild-type) and $\beta = 1.02 \text{ s}^{-1}$, $\beta_2 = 0.27 \text{ s}^{-1}$, $\sigma = 0.30$, $v_0 = 1.42 \mu\text{m/s}$ (NHE-deficient). For the other case we obtain $\beta = 0.70 \text{ s}^{-1}$, $\kappa = 0.017 \text{ s}^{-1}$, $\langle v \rangle = 0.83 \mu\text{m/s}$, $\langle v^2 \rangle = 2.92 \mu\text{m}^2/\text{s}^2$ (wild-type) and $\beta = 0.14 \text{ s}^{-1}$, $\kappa = 0.011 \text{ s}^{-1}$, $\langle v \rangle = 0.49 \mu\text{m/s}$, $\langle v^2 \rangle = 1.01 \mu\text{m}^2/\text{s}^2$ (NHE-deficient).

Figure 4.

VACF comparison between the results from the stick-slip model presented here (solid lines), the models A and B (dotted lines) and the experimental data for AX4 strains of *Dictyostelium* cells obtained in [11] (asterisks). The fitted parameters are, for the stick-slip model, $\beta = 1.20 \text{ s}^{-1}$, $\beta_2 = 1.08 \text{ s}^{-1}$, $\sigma = 0.41$, $v_0 = 5.43 \mu\text{m/s}$. For the models A and B we obtain $\beta = 2.07 \text{ s}^{-1}$, $\kappa = 0.10 \text{ s}^{-1}$, $\langle v \rangle = 4.95 \mu\text{m/s}$, $\langle v^2 \rangle = 63.2 \mu\text{m}^2/\text{s}^2$.

Figure 5.

Comparison for the kurtosis between models A (left) and B (middle), and the

stick-slip model presented here (right), for different (arbitrary) values of the parameters. For the speed distributions we have taken for simplicity a double Dirac delta $\frac{1}{2} [\delta(\langle v \rangle + v_D) + \delta(\langle v \rangle - v_D)]$ (the values of the parameters are given in the legend). The dashed line denotes a value of the kurtosis equal to 3 (Gaussian variable). This relatively complex behavior is in contrast with the monotonic growth one finds for the OU process.

Figure 6.

Comparison between the values of the kurtosis obtained from the stick-slip model (solid lines), the model A (dotted lines) and the experimental data extracted from [8] for vegetative and starved *Dictyostelium* cells (symbols). The values of the parameters are the same as those adjusted in Figure 2.

Figure 2

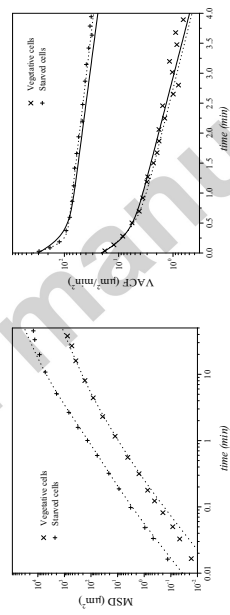


FIGURE 3

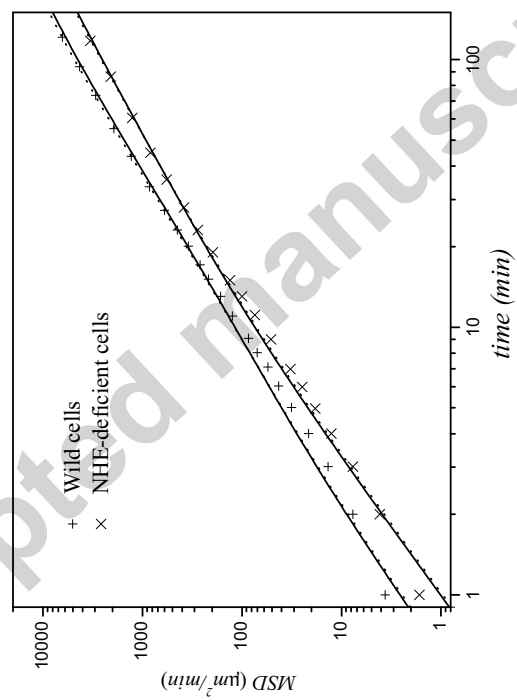


FIGURE 4

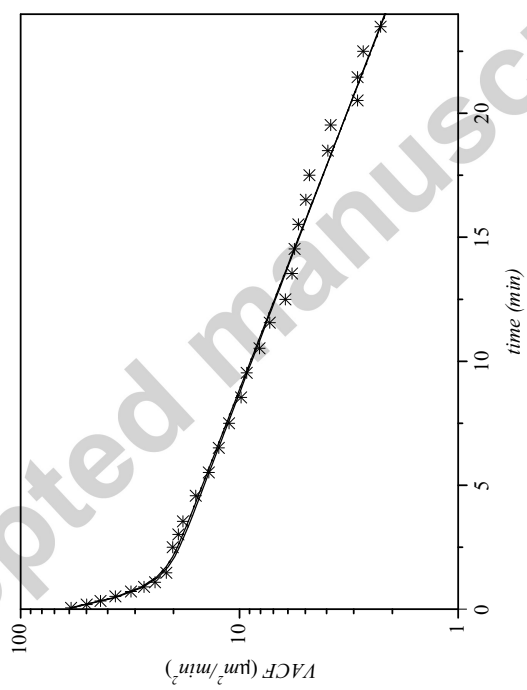


FIGURE 5

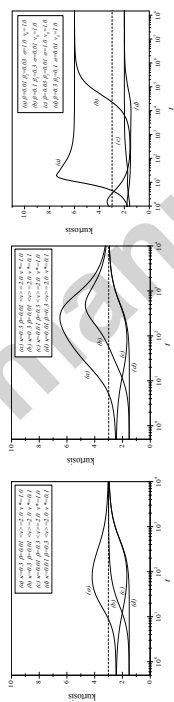


FIGURE 6

